Published in final edited form as:
Nat Cell Biol. ; 13(11): 1315–1324. doi:10.1038/ncb2340.

SHARPIN is an endogenous inhibitor of beta1-integrin activation

Juha K. Rantala[1,*], **Jeroen Pouwels**[1,2,*], **Teijo Pellinen**[1,2], **Stefan Veltel**[1,2], **Petra Laasola**[1], **Christopher S. Potter**[3], **Ted Duffy**[3], **John P. Sundberg**[3], **Olli Kallioniemi**[1,4], **Janet A. Askari**[5], **Martin Humphries**[5], **Maddy Parsons**[6], **Marko Salmi**[7], and **Johanna Ivaska**[1,2,8]

[1]Medical Biotechnology, VTT Technical Research Centre of Finland, 20521, Turku, Finland [2]Centre for Biotechnology, University of Turku, 20520, Turku, Finland [3]The Jackson Laboratory, Bar Harbor, ME, USA [4]Institute for Molecular Medicine Finland (FIMM), Biomedicum 2U, University of Helsinki, 00014 University of Helsinki, Helsinki, Finland [5]Wellcome Trust Centre for Cell-Matrix Research, Faculty of Life Sciences, University of Manchester, United Kingdom [6]Randall Division of Cell and Molecular Biophysics, King's College London Guy's Campus, London, SE1 1UL, UK [7]MediCity Research Laboratory and Department of Medical Biochemistry and Genetics, University of Turku, and National Institute for Health and Welfare, FIN-20520 Turku, Finland [8]Department of Biochemistry and Food Chemistry, University of Turku, 20520, Turku, Finland

Abstract

Regulated activation of integrins is critical for cell adhesion, motility and tissue homeostasis. Talin and Kindlins activate β1-integrins, but the counteracting inhibiting mechanisms are poorly defined. Here we identified SHARPIN as an important inactivator of β1-integrins in an RNAi-screen. SHARPIN inhibited β1-integrin functions in human cancer cells and primary leukocytes. Fibroblasts, leukocytes and keratinocytes from SHARPIN-deficient mice exhibited increased β1-integrin activity which was fully rescued by re-expression of SHARPIN. SHARPIN directly bound to a conserved cytoplasmic region of integrin α-subunits and inhibited recruitment of Talin and Kindlin to the integrin. Therefore, SHARPIN inhibits the critical switching of β1-integrins from inactive to active conformations.

Introduction

Integrins are heterodimeric transmembrane proteins composed of α- and β-subunits which mediate cell-cell and cell-extracellular matrix (ECM) adhesions[1]. The affinity of integrins for their ligands (integrin activation) is allosterically regulated [2–4]. Regulation of integrin activity is fundamentally important during development and in many physiological processes in adults [2, 3, 5–8]. It is now widely accepted that binding of cytoplasmic proteins Talins (TLN1,2) and Kindlins (FERMT1-3, fermitin family member 1–3) to the cytoplasmic tail of integrin β-subunit is critical for integrin activation [2, 9]. However, molecules capable of inactivating integrins are not well characterized for the β1-integrins.

Correspondence should be addressed to JI, Johanna.ivaska@vtt.fi.
*equal contribution.

Contributions

J.K.R. and O.K. developed CSMA, J.K.R. and T.P. performed the screen. J.K.R., J.P., P.L. S.V. and J.I, performed the experiments. M.P. performed the FRET-FLIM, C.S.P, T.D. and J.S. contributed to the mouse data, J.A.A and M.H. contributed to the LT integrin experiments, and M.S. contributed to the leukocyte work. J.P, J.I and M.S. wrote the manuscript.

SHARPIN is a 45 kDa cytosolic protein, originally identified in the postsynaptic density of excitatory synapses in brain, where it binds Shank-proteins [10]. We identified SHARPIN as a widely expressed endogenous inhibitor of β1-integrin activity.

Results

An RNAi screen identifies SHARPINs as an inhibitor of β1-integrin activity

To uncover proteins that function as endogenous inhibitors of β1-integrin (ITGB1) activity, we performed a high-throughput RNAi screen in PC3 prostate cancer cells using a Qiagen Kinase-Phosphatase siRNA library, targeting 897 known or putative genes encoding human kinases, phosphatase and certain other proteins. As integrin activation involves profound conformational changes, specific monoclonal antibodies can be used to detect β1-integrin activation [11]. Cells were transfected by growing them on microarrays of siRNA containing matrix spots. Subsequently, the cells were fixed and stained with 12G10 (an active β1-integrin conformation specific mAb [11]), fluorescently labelled phalloidin (for determination of cell area) and a DNA stain (for normalization of cell numbers). Samples were then analyzed using automated microscopy (Fig. 1a–b). Negative control siRNA and two validated siRNAs for *ITGB1* (β1-integrin gene) were used as negative and positive controls, respectively (Supplementary Fig. S1a). As binding of 12G10 may influence integrin conformation in live cells, it was critical to use fixed cells. Importantly, the specificity of the 12G10 antibody for β1-integrin was retained also in fixed cells since staining was lost upon β1-integrin silencing (Supplementary Fig. S1b).

In the screen, 44 siRNAs (2.5% hit rate) induced a significant increase in active integrin expression (z-score greater than +2SD) (Fig. 1b). Each gene was targeted by two independent siRNAs and for 5 genes both siRNAs (see Supplementary Table S1 for siRNA sequences) significantly increased integrin activation. Four of these target genes have been directly or indirectly linked to regulation of cell adhesion (Fig. 1b, red columns): *PRKAA2* (encoding AMPKα2) [12, 13], *EPHB2* [14–16], and members of the PKC-family (*PRKCD* codes for PKCδ and *PRKCH* for PKCη) [17, 18]. In contrast, SHARPIN has not been described to regulate cell adhesion or integrin function earlier.

SHARPIN regulates integrin activity in cancer cells

SHARPIN has been detected in brain, spleen, lungs [10], and certain cancer types [19]. We found SHARPIN to be rather broadly expressed at different protein/mRNA levels in several human cancer cell types and most normal tissues (Supplementary Fig. S1c, d).

Endogenous SHARPIN localized to membrane ruffles, the cytosol and the nucleus and this localisation was not influenced by GFP- or MYC-tags on the proteins (Supplementary Fig. S1e). Two different siRNAs against *SHARPIN* effectively knocked down the protein in PC3 cells (Fig. 1c). In line with the siRNA screening results, active β1-integrin staining (12G10) was increased (24±4% for siRNA1 and 19±3% for Smart pool siRNA) in cells transfected with the two different *SHARPIN* siRNAs (Fig. 1d), whereas the total amount of β1-integrin, detected by mAb K20 [11], was not altered (Supplementary Fig. S2a). A second mAb recognizing another epitope specific for the active conformation of β1-integrin (9EG7) [11], also displayed significantly increased staining of *SHARPIN* silenced cells. Conversely, over-expression of SHARPIN in PC3 cells decreased both 12G10 and 9EG7 staining (Fig. 1c, d). Importantly, integrin activation was similar in *SHARPIN* silenced cells and in cells overexpressing Talin-head, a construct sufficient for integrin activation [20] (Supplementary Fig. S2b). Furthermore, silencing of Talin reduced β1-integrin activity to a similar extent than overexpression of GFP-SHARPIN (Supplementary Fig. S2b).

SHARPIN silencing also induced significant changes in the levels of active and inactive β1-integrins on the cell surface as detected by flow cytometry. Silencing of *SHARPIN* increased 12G10 and 9EG7 and reduced Mab13 and 4B4 stainings (two mAbs specific for inactive β1-integrin [11]) but did not markedly alter total surface β1-integrin levels on the cell (Fig. 1e, Supplementary Fig. S2c, d). Importantly, the ability of *SHARPIN* siRNAs to increase β1-integrin activity was specifically due to loss of SHARPIN protein rather than off-target effects since transfection of *SHARPIN*-silenced cells with siRNA resistant GFP-SHARPIN significantly decreased β1-integrin activity compared to GFP transfected control cells (Fig. 1f).

Also in NCI-H460 human non-small cell lung cancer cells silencing of *SHARPIN* resulted in significant increase of β1-integrin activity as detected by increased 9EG7 and decreased Mab13 staining on the cell surface (Supplementary Fig. S2e–f). Taken together, these data indicate that SHARPIN functions as an inhibitor of β1-integrin activity in human cancer cell lines.

SHARPIN regulates ligand binding and migrationof cells

Inside-out activation of integrins induces ligand binding, cell adhesion and migration [21]. We found that *SHARPIN* silencing enhanced integrin binding of Alexa647-labelled fibronectin repeat 7–10 (FN7-10) (Fig. 1g), which harbours the integrin binding RGD-motif [22]. In addition, *SHARPIN* silencing induced cell adhesion to fibronectin (Fig. 1h). Cell migration is dependent on matrix concentration and receptor activity (following a bell-shaped response curve) [23]. Time-lapse imaging and tracking showed that silencing of *SHARPIN* significantly increased the speed of cell migration only on low matrix concentrations (Fig. 1i). Finally, reduction of integrin activity by overexpression of GFP-SHARPIN significantly decreased cell motility on plastic (Fig. 1j) whereas transfection with two different *SHARPIN* siRNAs significantly increased cell motility (Supplementary Fig. S2g). These assays demonstrate that SHARPIN functionally inhibits ligand binding to β1-integrins and β1-integrin mediated cellular functions consistent with its ability to inhibit activation of β1-integrin.

SHARPIN interacts with the cytoplasmic domain of integrin α-subunits

All well-characterized regulators of integrin activity, like activators Talins and Kindlins and integrin inhibitors, such as Filamin (FLN) and docking protein 1 (DOK1), function via interaction with the integrin β-subunit [24, 25]. However, in pull-down experiments with biotinylated peptides of the cytoplasmic domains of β1, α1- (ITGA1), and α2-integrins (ITGA2) (Fig. 2a) we unexpectedly found that MYC-tagged SHARPIN bound to α1- and α2-tail peptides, but not to the β1-cytoplasmic tail (Fig. 2b). The interaction was seen when the α-tail peptides contained the conserved membrane proximal segment found in all integrin α-subunits (α2-cons), whereas binding to the α2-tail lacking this sequence (α2-cterm) was at background levels (Fig. 2b). Importantly, endogenous SHARPIN also bound to the α-conserved tail but not to the β1-tail (Fig. 2c). Thus SHARPIN associates with the cytoplasmic domain of integrin α-subunits.

Pull-down experiments with recombinant, purified GST-SHARPIN and biotinylated integrin tail peptides (Fig. 2d), revealed that GST-SHARPIN bound directly to the α2-tail but not the β1-tail (recombinant Talin 1–400 fragment [26] was used as a positive control for the β1-tail pulldown). Based on fluorescence polarization titrations between GST-SHARPIN and the α-conserved tail, the affinity of the interaction was 26±5 μM (α2-wt; five α2-specific C-terminal amino acids were included to obtain solubility and to ensure proper folding) (Fig. 2e). Alanine scanning mutations within the integrin α-tail conserved segment revealed that SHARPIN binding is mainly mediated by residues WK, LG and FF (Fig. 2e). The conserved arginine (residue 8 of the peptide) may form an inhibitory salt-bridge with the integrin β1-

subunit [27]. If SHARPIN bound to this residue, it could disrupt the salt-bridge and activate rather than inactivate integrins. Notably, in line with the inhibitory effect of SHARPIN on integrin activity, SHARPIN interaction with integrin α-tail did not require arginine 8 in the peptide.

The specificity of the pull-down experiments was corroborated with additional controls. GST-SHARPIN did not interact with scrambled α2-peptide (amino acids from α2-cons peptide in random order) or mutated α2-34AA-tail or β1-tail (Fig. 2f). In addition, the interaction between GST-SHARPIN and α2-cons was partially competed by excess non-biotin labeled α2cons peptide but not β1-tail peptide. Finally, in cells GFP-SHARPIN was found to co-precipitate with α2- and α5-cytoplasmic tails, but not the β1-tail, fused to the extracellular and transmembrane parts of ILR2α TAC subunit [28, 29] (Fig. 2g). This demonstrates that the integrin α-subunit binding sequence interacts with SHARPIN even when inserted into an irrelevant transmembrane protein. Taken together, these experiments show that SHARPIN directly binds to the conserved region of the cytoplasmic domain of several α-integrins.

SHARPIN co-localizes and interacts with β1-integrin in cells

Next we studied whether SHARPIN and integrins can also physically interact in intact cells. We found that SHARPIN localizes to the cytoplasm and membrane ruffles at the cell periphery of NCI-H460 cells (Fig. 3a). SHARPIN was found to co-localize with inactive β1-integrin in these ruffles in non-transfected (Fig. 3a) and control siRNA transfected cells (Fig. 3b left), whereas the ruffles were absent from the more spread *SHARPIN*-silenced cells (Fig. 3b, right). In contrast, active β1-integrin predominantly localized to the substrate-facing matrix adhesions and did not colocalize with SHARPIN (Fig. 3a). These data show that SHARPIN co-localizes with inactive β1-integrins in cells, and are consistent with its role in inactivating integrins that mediate cell adhesion to the matrix.

In co-immunoprecipitation experiments from PC3 cells grown on plastic (Fig. 3c), SHARPIN co-precipitated strongly with α2β1-integrin and, to a lesser extent, with α5β1-integrin when monospecific anti-integrin antibodies (Supplementary Fig. S3) were used for the immunoprecipitation. On plastic, cell adhesion is mediated predominantly via α5β1 binding to fibronectin while the collagen binding α2β1 integrin is unoccupied and potentially more shifted to the inactive conformation. Therefore, we compared the amounts of SHARPIN that coimmunoprecipitate with α2- and α1-integrins from cells in suspension and from cells adhering to their substrate collagens (Fig. 3d, e). SHARPIN coimmunoprecipitated more strongly with α-integrins from cells in suspension indicating that SHARPIN (preferentially) binds unoccupied/inactive integrins. Importantly, α5-integrin WT co-precipitated SHARPIN more effectively than α5-integrin 34AA (Fig. 3f), in which two of the SHARPIN-binding residues were mutated into alanines (see Fig. 2e).

We also analyzed the direct interactions between co-expressed GFP-SHARPIN and α5-integrin-mcherry by fluorescence resonance energy transfer (FRET) using fluorescence lifetime imaging microscopy (FLIM) [30]. Direct binding between SHARPIN and α5-integrin (FRET efficiency 7.2±1.4%, n=12) was clearly seen in analyses of FRET lifetime images and cumulative FRET efficiency data (Fig. 4a). Collectively these experiments demonstrate that SHARPIN directly interacts with multiple α-subunits, preferentially in their inactive conformation, in intact cells.

SHARPIN inhibits recruitment of Talin and Kindlin to β1-subunits

SHARPIN could inactivate integrins by modulating the expression and/or function of the β1-integrin activators Talin [3, 31] or Kindlin [22, 32–34] or via LUBAC stimulated formation of

linear ubiquitin chains involved in signalling [35–37]. We found that silencing of SHARPIN did not alter protein levels of Talin or Kindlin (Supplementary Fig. S4a). Furthermore, silencing of *HOIP* (RNF31, the catalytic subunit of LUBAC) did not induce β1-integrin activity in cells (Supplementary Fig. S4b). To test whether binding of SHARPIN to integrin α-tails directly or indirectly inhibits binding of Talin and/or Kindlin to β1-integrin, we performed two assays. First, direct binding of mcherry-Talin1 or mcherry-Kindlin2 to β1-integrin-GFP was measured using FRET-FLIM in β1-integrin knock-out MEF cells transfected with MYC-SHARPIN or control plasmid. Comparison of FRET lifetime images and FRET efficiency data showed a very significant reduction in the interaction between β1-GFP and mcherry-Talin and β1-GFP and mcherry-Kindlin2 in cells positive for MYC-SHARPIN (Fig. 4b, c). Second, the ability of SHARPIN to influence the interaction between β1-integrin and Kindlin was studied using proximity ligation assay (PLA) [38, 39]. The modest PLA signal detectable at the periphery of control cells (Fig. 4d), indicating interaction between β1-integrin and Kindlin2, was very significantly increased in *SHARPIN*-silenced cells (PLA signals per cell 18±2 in control and 61±17 in *SHARPIN* siRNA cells (n=274 cells, $p<0.001$) (Fig. 4d).

Silencing of *Sharpin* in β1-null GD25 mouse cells transfected with human WT full-length α5β1 integrin increased binding of SNAKA51 mAb, which only detects active human α5β1 integrin [40]. In contrast, *SHARPIN* silencing had no effect on the low SNAKA51 labelling of transfected full-length human α5β1 legs-together (LT) mutant, in which the subunits are restrained together (thus preventing inside-out activation) (Fig. 4e).

Together these data suggest that endogenous SHARPIN strongly inhibits (directly or indirectly) the β1-integrin-Talin and β1-integrin-Kindlin interaction in cells. Therefore, the inside-out integrin activation is dynamically controlled by the balance of counteracting forces exerted by SHARPIN and Talin/Kindlin.

SHARPIN regulates β1-integrin activity in primary leukocytes

We then studied whether SHARPIN also regulates β1-integrin activity in non-adherent primary cells. Freshly isolated human peripheral blood leukocytes (PBL) expressed clearly detectable levels of SHARPIN protein (Fig. 5a). Silencing of *SHARPIN* in these primary cells resulted in a marked increase in β1-integrin mediated spreading and migration on fibronectin coated surfaces (Fig. 5b, c) without influencing cell surface levels of α4-, α5- or β1-subunits (Fig. 5d). In addition, *SHARPIN* silencing in PBL resulted in increased active β1-integrin levels on the plasma membrane compared to control siRNA transfected cells. Importantly, this effect was reversed by expression of siRNA resistant GFP-SHARPIN (Fig. 5e). Finally, overexpression of GFP-SHARPIN in PBL resulted in a significant reduction in β1-integrin activity on the plasma membrane as detected by antibodies against active and inactive conformations of β1-integrin (Fig. 5f). These data revealed that SHARPIN also acts as an inhibitor of β1-integrin activation in non-malignant primary cells, and controls leukocyte adhesion and migration.

SHARPIN controls β1-integrin activity *in vivo*

Mice harbouring a spontaneous null-mutation in the *Sharpin* gene (C57BL/KaLawRij-*Sharpin*^{cpdm}/RijSunJ, abbreviated to *cpdm*) display multiorgan inflammation and eosinophilic proliferative dermatitis [41, 42]. Recently, the phenotype has been associated with deregulation of the NF-kB activity due to impaired linear ubiqitination [35–37], albeit mice lacking another subunit of LUBAC, HOIL-1 (RBCK1), do not have a similar phenotype [43]. We investigated whether increased integrin activity could also be detected in cells and tissues from the SHARPIN null mice. *cpdm* mice had significantly higher levels (5.1±0.6-fold total fluorescence intensity, n=9 sections, $p<0.001$) of active β1-integrin (9EG7

labelling) compared to wild-type control mice (Fig. 6a). In *cpdm* mice, the increased β1-activity was mainly detected in keratin 14 (KRT14) positive keratinocytes and less in supra-basal keratinocytes positive for keratin 10 (KRT10) or involucrin (IVL) (Fig. 6a). Increased β1-integrin activity in *cpdm* mice was not accounted for by changes in the expression of *ITGB1* or any of *Kindlin* or *Talin* genes in the skin (Supplementary Table S2, microarray data published in [41]).

Freshly isolated splenocytes from *cpdm* mice displayed 450% increased active cell surface β1-integrin (9EG7) and 200% increased fibronectin-fragment binding compared to WT splenocytes (Fig. 6b). Increased integrin activity was also detected in bone marrow leukocytes freshly isolated from *cpdm* mice compared to the corresponding WT cells (Fig. 6c). These analyses show that loss of SHARPIN correlates with increased β1-integrin activity also *in vivo*. However, we can not conclude that this is directly due to the loss of the integrin inhibitory role of SHARPIN since the inflammation in the *cpdm* mice might influence integrins indirectly.

Mouse embryonic fibroblasts (MEFs) from WT and *cpdm* embryos (at a stage with no detectable inflammation) were analyzed for FN7-10 binding. Notably, SHARPIN null MEFs displayed 1.7–2.5–fold increased β1-integrin ligand binding with similar levels of total cell surface β1-integrin (Fig. 6d–e), thus demonstrating a significant increase in β1-integrin activity compared to wild-type MEFs. The increase was specifically due to loss of SHARPIN, since re-expression of SHARPIN in the *cpdm* MEFs fully reversed the phenotype (Fig. 6e). In addition, *cpdm* MEFs were more migratory than WT MEFs on plastic, which was reversed upon expression of GFP-SHARPIN (Fig. 6e).

Importantly, the ability of SHARPIN to inhibit integrin activity was found to depend on its ability to interact with the integrin α-subunit. This was shown by staining WT and *cpdm* MEFs expressing human α5-GFP wt or α5-GFP 34AA with SNAKA51. WT-α5-integrin activity was 1.8-fold higher in *cpdm* MEFs compared to WT MEFs. In contrast, in cells transfected withα5-integrin 34AA, which is unable to interact with SHARPIN, SNAKA51 detected similar levels of active α5-integrin both in SHARPIN expressing WT cells and SHARPIN null *cpdm* cells (Fig. 6f). In addition, a membrane-permeable soluble α-tail peptide (containing the SHARPIN binding sequence) had no effect in GFP transfected *cpdm* MEFs but significantly blocked the ability of GFP-SHARPIN to reduce integrin activity in *cpdm* MEFs, whereas a scramble control peptide had no effect (Fig. 6g). Together these data show that loss of SHARPIN correlates with increased integrin activity *in vivo* and that in cells this is dependent on its ability to interact with integrin α-subunit.

Discussion

Our study demonstrates that SHARPIN inactivates integrins in many cell types and influences integrin dependent cellular functions. It switches integrins into an inactive conformation by directly interacting with the conserved membrane proximal segment present in all integrin α-subunits. This interaction results in reduced recruitment of integrin activators Talin and Kindlin to the β1-subunit. In addition, loss of SHARPIN correlates with increased β1-integrin activity *in vivo.*

Filamin and DOK1 inhibit β1-integrin in cells by binding to the β-cytoplasmic tails and competing directly with Talin binding [24, 25, 44, 45]. SHARPIN, in contrast, inhibits β1-integrin activity by binding directly to the α-subunits. SHARPIN, in contrast, inhibits β1-integrin activity by binding directly to the α-subunits and its expression correlates with the low-affinity conformation of β1-integrins *in vivo*. We recently showed that mammary derived growth inhibitor (MDGI) can function as a negative regulator of β1-integrins in

breast cancer [46] but overexpression or knock-down of MDGI has no detectable phenotype *in vivo* [47]. In contrast, SHARPIN inhibits integrin activity in many cell types and loss of SHARPIN correlates with increased β1-activity in *cpdm* mice. Thus, SHARPIN can serve as a general inhibitor of β1-integrins. Identification of this function of SHARPIN opens up an interesting concept in integrin regulation by showing that the dynamic switching between inactive and active conformations [1, 3, 48] is physiologically controlled by a protein interacting with the α-subunits.

SHARPIN has been shown to bind to PTEN and inhibit its lipid phosphatase activity [49] and to enter into the nucleus and function as a transcription co-activator of EYA-1 [50]. We show here that the ability of SHARPIN to inactivate integrins is independent of these functions since *SHARPIN* silencing induces integrin activation in PC3 cells, which are PTEN null [51] and which also lack EYA-1 expression (Affimetric scale expression < 50) [52]. In addition, our data demonstrate that SHARPIN interaction with the integrin α-tail is necessary for integrin inactivation (Fig. 6f–g). We found that SHARPIN is not able to rescue the phenotype of *cpdm* MEFs in the presence of a competing soluble α-chain peptide. Furthermore, we found that the activity of a mutant α5 integrin (α5-34AA, which does not interact with SHARPIN) is not increased by deletion of SHARPIN, in contrast to the activity of wild-type α5 integrin. SHARPIN also functions as a subunit of LUBAC which stimulates linear ubiquitin chain assembly [35–37]. However, recombinant SHARPIN (in the absence of HOIP and HOIL-1) interacts with the integrin α-tail in an ubiquitin independent manner (as we detect binding to synthetic peptides). In addition, silencing of HOIP (the catalytic subunit of LUBAC) has no effect on integrin activity in cells (Fig. S4b). Moreover, about half of cellular SHARPIN is not associated with the LUBAC complex [37]. Therefore, we conclude that SHARPIN is a multifunctional molecule, which also binds directly to integrin α-subunits and inactivates integrins independently of its other functions in cells. However, these data open an intriguing additional possibility whereby recruitment of LUBAC to the integrins would catalyse linear ubiqitination of components of the adhesome and influence their function.

Already in the early 90's it was speculated that if an association between a protein and the α-integrin GFFKR-sequence would occur, it may determine the default affinity state of the integrin. This hypothesis was based on a finding that deletion of the integrin α-tail before this sequence results in a constitutively active integrin [53]. We now present evidence that SHARPIN functions as such a protein in many different cell types.

In conclusion, SHARPIN is an endogenous inhibitor of β1-integrins, which uniquely binds to α-integrin subunits. It can function either via holding the integrins in an inactive state (by steric hindrance of the binding of Talin and Kindlin or by stabilizing the salt-bridge) or via serving as an adaptor recruiting inhibitory kinase(s) to the proximity of β-chains. In any case, SHARPIN prevents interaction of β1-integrin with Talin and Kindlin. SHARPIN controls β1-integrin dependent cell adhesion and migration in several normal and malignant cell types and loss of SHARPIN correlates with increased integrin activity in mice *in vivo*.

Methods

Cell spot microarrays (CSMA)

For the siRNA cell spot microarrays a library with two individual siRNAs for 897 human kinases and phosphatases and certain other genes (Qiagen kin-phos library v1.0), ITGB1 (SI00300573, SI02662044) and negative control siRNAs (All star negative control, Qiagen 1027280, siGFP, Qiagen 1022064) were printed on a SBS-sized untreated polystyrene microplate (Nunc) using a Genetix Qarray2 (Genetix Ltd) microarray printer with 200 μm solid tip pins (PointTechnologies) as described earlier [54]. PC-3 cells were transfected on the

arrays for 48 h, fixed with 2% paraformaldehyde, permeabilized with 0.3% Triton-X100 in PBS and stained with an antibody specific for active β1-integrin (clone 12G10, 1:100), Alexa555 conjugated phalloidin (Invitrogen, 1:50) and DAPI. Alexa488 conjugated goat anti-mouse secondary antibody was used (1:300) to detect the primary antibody. Analysis of the arrays was performed with an automated HTP fluorescence microscope (ScanR, Olympus) using 20x objective. Automated image analysis (ScanR, Olympus) was used to measure a cumulative F-actin segmented whole cell area, anti-12G10 signal intensity and nuclear DNA counterstaining of all cells in each spot. The raw signal intensities were spatially centred using pin normalization and the ratio of fitted signals (12G10/DAPI) was standardized with a z-score using whole array mean and standard deviation.

Immunofluorescence

For FACS analysis the cells were stained with the indicated integrin antibodies (1:100) followed by fluorescently conjugated secondary antibodies (1:300), as described [46]. For analysis of the binding of labeled fibronectin repeat 7–10 (FN) [22], non-fixed cells suspended in Tyrodes buffer (10 mM Hepes-NaOH pH 7.5, 137 mM NaCl, 2.68 mM KCl, 0.42 mM NaH_2PO4, 1.7 mM $MgCl_2$, 11.9 mM $NaHCO_3$, 5 mM glucose) were incubated with the ligand (25 μg/ml) for 30 min at room temperature, washed 3 times with cold Tyrodes and analysed by FACS. Immunofluorescence experiments were performed as described [39]. For analysis of integrin activity in the 96 well plates the transfected cells were fixed, permeabilized and stained for active integrins (9EG7 and 12G10, both 1:100) or total integrin (K20 or P5D2, both 1:100) and DAPI, followed by fluorescently conjugated secondary antibodies (1:300). Samples were imaged using ScanR microscope (Olympus) and a 20x objective and quantitated using ScanR image analysis software.

Dorsal skin samples from 6 week old wild-type and C57BL/KaLawRij-*Sharpin*^{cpdm}/RijSunJ mice were embedded in OCT, frozen, sectioned, fixed with 2% paraformaldehyde and stained with the indicated primary antibodies (1:100) and DAPI, followed by fluorescently conjugated secondary antibodies (1:300). Images were taken by a Zeiss LSM710 spinning disc confocal microscope (CarlZeiss) and a 20x objective.

Cell adhesion and migration assays

For migration assays subconfluent cells or cells at the edge of a scratch-wound were imaged at 10 min intervals in 10% FBS containing medium on 0.1, 5 or 50 μg/ml collagen coated wells (PC3) or tissue culture plates (MEFs) for 16 h, or on 5 μg/ml fibronectin coated wells at 1 minute intervals for 30 minutes (PBL). Phase-contrast images were taken with a Zeiss inverted wide-field microscope (10x objective) equipped with a heated chamber (37 °C) and CO_2 controller (4.8 %). Image processing was done with NIH ImageJ software. Migration was analysed by measuring the migration speed and path length.

Immunoprecipitations and pull-downs

Cell lysates were subjected to immunoprecipitations using the indicated antibodies (2 μg) at +4 °C overnight. Protein-G beads (GE Healthcare) in lysis buffer were added and incubated for 1 h at +4 °C. Beads were washed and suspended into loading buffer. Samples were separated in SDS-PAGE and analysed using Western blotting.

Biotin-conjugated and unlabelled peptides were from Genecust. For pull-down analysis, the cells were lysed in a lysis buffer (50 mM Tris pH 7.5, 2 % β-octylglycoside, 10 % glycerol, 300 mM NaCl, 1 mM DTT) with protease and phosphatase inhibitor cocktails. The lysates were incubated with equimolar concentrations of (2.5 μM) biotinylated integrin-peptides bound to streptavidin-sepharose beads. After washings, the bound proteins were detected by Western blot analysis. Similar experiments were performed with recombinant GST-

SHARPIN and Talin1–400 fragment (instead of cell lysates). In the competition experiments, 25 μM unlabelled peptides were added.

Protein interaction analysis using fluorescence polarization

For the polarization assay WT and alanine scanning mutant EDANS-labelled α2-peptides (Genscript) were used. We incubated 5 μM of these peptides with serial concentrations of GST-SHARPIN in 20 mM Tris, pH 6.8, 50 mM NaCl, 3 mM β-mercaptoethanol, 0.001% Tween20. Samples were analysed in a 384-well plate format in an ENVISION 2100 multi-label plate reader (Perkin Elmer) using 355 nm excitation and 500 nm emission filter. Data analysis, fitting, and plotting were done with Grafit 6.0 (Erithracus software). K_d values were calculated as described [55].

Antibodies

The following antibodies were used in this study (including dilutions/amounts used for immunofluorescence (IF), Western blot (WB) or immunoprecipitation (IP)): 12G10 (active integrin β1 [11], human specific, abcam; 1:100 IF), 9EG7 (active integrin β1 [11], mouse and human; BD Pharmingen; 1:100 IF), SNAKA51 (human specific active integrin α5β1 [56]; 1:100 IF), K20 (integrin β1 [11], Immunotech; 1:300 IF), AIIB2 (integrin β1, Drosophila Studies Hybridoma Bank; 1:1000 WB), Mab13 (inactive integrin β1 [11], BD Pharmingen; 1:100 IF), 4B4 (inactive integrin β1 [11], Beckman Coulter; 1:100 IF), MB1.2 (integrin β1, mouse specific, Millipore; 1:100 IF), 1934 (integrin α1, Chemicon; 1:1000 WB, 2 μg IP), 1936 (integrin α2, Chemicon; 1:1000 WB, 2μg IP), 16983 (integrin α4, Chemicon; 1:100 IF), 1949 (integrin α5, Chemicon; 1:100 IF, 1:1000 WB, 2 μg IP), SHARPIN (ab69507, Abcam; 1:100 IF, 1:300 WB), Kindlin (pan)(ab68041, Abcam; 1:100 IF), GFP (A11122, molecular probes; 1:1000 WB, 2 μg IP), MYC (ab9106, Abcam; 1:1000 WB), Tubulin β (ab6160, Abcam; 1:1000 WB), GST (91G1, Cell Signal. Tech.; 1:1000 WB), Talin 1/2 (H-300, Santa Cruz Biotech.; 1:1000 WB), Keratin 10 (PRB-155P, Biosite; 1:100 IF), Keratin 14 (PRB-159P, Biosite; 1:100 IF), Involucrin (PRB-140C, Biosite; 1:100 IF), RNF31/HOIP (ab46322, Abcam; 1:1000 WB), TAC (IL-2Rα, sc-664, Santa Cruz Biotech.; 1:200 WB, 2 μg IP).

Cells

PC3 cells were grown in RPMI 1640 medium supplemented with 1% L-glutamine, 10% fetal bovine serum (FBS), and 1% penicillin-streptomycin. NCI-H460 human non-small cell lung cancer cells were grown in RPMI 1640 medium supplemented with 1% HEPES buffer, 1% L-glutamine, 1% sodium pyruvate, 10 % FBS and 4500 mg/l glucose. The β1-GFP expressing β1-knockout MEFs were generated as described earlier [30] and were grown in DMEM containing 10% FCS and penicillin, streptomycin, glutamine and 20 U/ml IFN-γ (all from Sigma) at 33 °C. The GD25 cells were a kind gift from R. Fassler (Max Planck Institute of Biochemistry, Martinsried, Germany). MEFs were isolated from WT and SHARPIN null (*cpdm*) mice according to standard methods [57], immortalized by retroviral infection of pBABE-Large T (Biomedicum Genomics, Helsinki, Finland) and grown in DMEM containing 10% FCS and penicillin, streptomycin, glutamine, sodium pyruvate, non-essential amino acids and 0.001% β-mercapto-ethanol (Sigma).

Mononuclear peripheral blood leukocytes were isolated from volunteers using Ficoll gradient centrifugation.

Mice were euthanized using CO_2 gas and heparinised venous blood was collected from the right ventricle. Erythrocytes were lysed with Gey's RBC Lysis Buffer and washed. From spleens cell suspensions were prepared by mechanical teasing. Bone marrow leukocytes were isolated from femurs by needle aspiration.

DNA constructs

The MYC-SHARPIN expression construct was a kind gift from S. Lee (Chungnam National University, Daejeon, Korea) [10]. For construction of GFP-SHARPIN the corresponding DNA fragments were amplified from Image clone 4737834 using specific primers introducing XhoI and XbaI sites and cloned into pEGFP-C1 (Clontech). The siRNA1-resistant GFP-Sharpin was made by mutating GFP-Sharpin using standard site directed mutagenesis using the following primer: CCTGGCCCCATCAGG**T**T**A**CA**A**GT**G**ACACTTGAAGACGCTGCC (silent mutations in bold). The GST-SHARPIN expression construct was made by amplification of *SHARPIN* from the GFP-SHARPIN expression vector using specific primers that introduce EcoRI and BamHI sites, followed by cloning into pGEX4T-1. The α5-GFP 34AA was obtained by mutating α5-GFP WT [58] using standard site directed mutagenesis. The constructs were verified with sequencing. Construction of β1-GFP [30], β1-CFP WT, β1-CFP legs together, α5-YFP WT and α5-YFP legs together [40] have been described previously. The mcherry-talin and α5-mcherry constructs were generous gifts from K. Yamada (National Institutes of Health, Bethesda, MD) and J. Norman (The Beatson Institute for Cancer Research, Glasgow, UK) [59], respectively. mcherry-kindlin2 was made by subcloning from EGFP-kindlin2, which was kindly provided by R. Fassler (Max Planck Institute of Biochemistry, Martinsried, Germany). TAC constructs were kindly provided by M. Ginsberg (UC San Diego).

RNAi transfections

Two different annealed siRNAs targeting human *SHARPIN* (*SHARPIN* ON-TARGETplus SMARTpool: CCGCAGTGCTCTTGGCTGT; GGAACTTGGACGCTTGTTT; GGTCACACTTGAAGACGCT; GTGGAAGGACAGAATGGCA (Dharmacon) and Hs_*SHARPIN*_1 HP siRNA: CAGGCTGCAGGTCACACTTGA (Qiagen)), mouse *Sharpin* (1:1:1:1 mix of Mm_0610041B22Rik_1 till 4 FlexiTube siRNA: CGGGTCCTTCTTGTTCTCCAA; GACAGAGATGCCAGTGTTAAA; TTCGTTCGAACCTTTAAGAAA; AAGCTAGTAATTAAAGACACA.

(Qiagen)), β1-integrin (Hs_ITGB1_5 FlexiTube siRNA: AAAAGTCTTGGAACAGATCTG and Hs_ITGB1_8: AAGAGGGATAATACAAATGAA (Qiagen)), α2-integrin (Hs_ITGA2_5 FlexiTube siRNA: CCCGAGCACATCATTTATATA (Qiagen)), α5-integrin (Hs_ITGA5_5 FlexiTube siRNA: ATCCTTAATGGCTCAGACAT (Qiagen)), Talin siRNAs: *TALIN1* and *TALIN2* (Hs_TLN1_2: CAGGGCAATGAGAATTATGCA and Hs_TLN2_1: CAGATGTTGTATGCAGCCAAA FlexiTube siRNA (Qiagen)), HOIP (Hs_RNF31, siRNA: GCAGAATACTCATCCAAGA (Qiagen)) or scramble control siRNA (AllStars Negative Control siRNA; Qiagen) were used. Transfections were performed using 200 nM siRNAs and Hiperfect (Qiagen) or human T cell nucleofector kit (Amaxa) according to the manufacturer's protocol and the cells were cultured for 2–3 days.

Protein expression and purification

Recombinant GST-SHARPIN was produced and purified in *E. coli* strain Rosetta BL21DE3 according to the manufacturer's instructions (BD Biosciences).

Skin whole tissue microarray analysis

Dorsal thoracic skin was collected and analyzed from 3 *cpdm* and 3 WT female mice at 2, 4 and 6 weeks of age to provide a cross sectional transcription profile of the *cpdm* phenotype using the GeneChip™ Mouse Gene 1.0 ST Arrays (Affymetrix), as previously reported [41].

Transcriptome data were evaluated for fold change, p and q values for the genes under investigation here.

FRET measurements by Fluorescence Lifetime Imaging Microscopy (FLIM)

Time-domain FLIM experiments and data analysis were performed as described previously [30].

Proximity Ligation Assay (PLA)

Proximity ligation assay detection of β1-integrin-kindlin interaction was performed according to a previously described protocol [38].

Statistical analysis

All statistical analyses were performed with Student's t-test. $p<0.05$ was considered significant.

Supplementary Material

Refer to Web version on PubMed Central for supplementary material.

Acknowledgments

We thank H. Marttila, J. Siivonen, L. Lahtinen, R. Kaukonen, E. Vaananen, K. Silva and A. Arola for excellent technical assistance. E. Mattila is acknowledged for MEF immortalization and PR. Elliot for the recombinant Talin1–400 protein. R. Fassler, M. Ginsberg, J. Norman and S. Lee are acknowledged for the plasmids. This study has been supported by Academy of Finland, EU-FP06 project ENLIGHT, ERC Starting Grant, Sigrid Juselius Foundation, EMBO YIP and Finnish Cancer Organizations. J.P. Academy of Finland postdoc grant, T.P. TUBS Graduate School and S.V. Alexander von Humbold foundation and EMBO LTF. C.P. and J.P.S were supported by the National Institutes of Health (T32 DK07449-28 to CP and AR49288 to JPS).

References

1. Hynes RO. Integrins: bidirectional, allosteric signaling machines. Cell. 2002; 110:673–87. [PubMed: 12297042]
2. Moser M, Legate KR, Zent R, Fassler R. The tail of integrins, talin, and kindlins. Science. 2009; 324:895–9. [PubMed: 19443776]
3. Shattil SJ, Kim C, Ginsberg MH. The final steps of integrin activation: the end game. Nat Rev Mol Cell Biol. 2010; 11:288–300. [PubMed: 20308986]
4. Larjava H, Plow EF, Wu C. Kindlins: essential regulators of integrin signalling and cell-matrix adhesion. EMBO Rep. 2008; 9:1203–1208. [PubMed: 18997731]
5. Margadant C, Charafeddine RA, Sonnenberg A. Unique and redundant functions of integrins in the epidermis. FASEB J. 2010; 24:4133–4152. [PubMed: 20624931]
6. Cantor JM, Ginsberg MH, Rose DM. Integrin-associated proteins as potential therapeutic targets. Immunol Rev. 2008; 223:236–251. [PubMed: 18613840]
7. Hogg N, Bates PA. Genetic analysis of integrin function in man: LAD-1 and other syndromes. Matrix Biol. 2000; 19:211–222. [PubMed: 10936446]
8. Evans R, et al. Integrins in immunity. J Cell Sci. 2009; 122:215–25. [PubMed: 19118214]
9. Calderwood DA. Integrin activation. J Cell Sci. 2004; 117:657–66. [PubMed: 14754902]
10. Lim S, et al. Sharpin, a novel postsynaptic density protein that directly interacts with the shank family of proteins. Mol Cell Neurosci. 2001; 17:385–397. [PubMed: 11178875]
11. Byron A, et al. Anti-integrin monoclonal antibodies. J Cell Sci. 2009; 122:4009–4011. [PubMed: 19910492]

12. Taliaferro-Smith L, et al. LKB1 is required for adiponectin-mediated modulation of AMPK-S6K axis and inhibition of migration and invasion of breast cancer cells. Oncogene. 2009; 28:2621–2633. [PubMed: 19483724]
13. Ewart MA, Kohlhaas CF, Salt IP. Inhibition of tumor necrosis factor alpha-stimulated monocyte adhesion to human aortic endothelial cells by AMP-activated protein kinase. Arterioscler Thromb Vasc Biol. 2008; 28:2255–2257. [PubMed: 18802013]
14. Guo DL, et al. Reduced expression of EphB2 that parallels invasion and metastasis in colorectal tumours. Carcinogenesis. 2006; 27:454–464. [PubMed: 16272170]
15. Huusko P, et al. Nonsense-mediated decay microarray analysis identifies mutations of EPHB2 in human prostate cancer. Nat Genet. 2004; 36:979–983. [PubMed: 15300251]
16. Zou JX, et al. An Eph receptor regulates integrin activity through R-Ras. Proc Natl Acad Sci U S A. 1999; 96:13813–13818. [PubMed: 10570155]
17. Ivaska J, et al. Integrin-protein kinase C relationships. Biochem Soc Trans. 2003; 31:90–3. [PubMed: 12546661]
18. Harper MT, Poole AW. Diverse functions of protein kinase C isoforms in platelet activation and thrombus formation. J Thromb Haemost. 2010; 8:454–462. [PubMed: 20002545]
19. Jung J, et al. Newly identified tumor-associated role of human Sharpin. Mol Cell Biochem. 2010
20. Calderwood DA, et al. The phosphotyrosine binding-like domain of talin activates integrins. J Biol Chem. 2002; 277:21749–21758. [PubMed: 11932255]
21. Schwartz MA, Assoian RK. Integrins and cell proliferation: regulation of cyclin-dependent kinases via cytoplasmic signaling pathways. J Cell Sci. 2001; 114:2553–60. [PubMed: 11683383]
22. Moser M, Nieswandt B, Ussar S, Pozgajova M, Fassler R. Kindlin-3 is essential for integrin activation and platelet aggregation. Nat Med. 2008; 14:325–330. [PubMed: 18278053]
23. Palecek SP, Loftus JC, Ginsberg MH, Lauffenburger DA, Horwitz AF. Integrin-ligand binding properties govern cell migration speed through cell-substratum adhesiveness. Nature. 1997; 385:537–40. [PubMed: 9020360]
24. Kiema T, et al. The molecular basis of filamin binding to integrins and competition with talin. Mol Cell. 2006; 21:337–347. [PubMed: 16455489]
25. Anthis NJ, et al. Beta integrin tyrosine phosphorylation is a conserved mechanism for regulating talin-induced integrin activation. J Biol Chem. 2009; 284:36700–36710. [PubMed: 19843520]
26. Elliott PR, et al. The Structure of the talin head reveals a novel extended conformation of the FERM domain. Structure. 2010; 18:1289–1299. [PubMed: 20947018]
27. Hughes PE, et al. Breaking the integrin hinge. A defined structural constraint regulates integrin signaling. J Biol Chem. 1996; 271:6571–4. [PubMed: 8636068]
28. LaFlamme SE, Akiyama SK, Yamada KM. Regulation of fibronectin receptor distribution. J Cell Biol. 1992; 117:437–447. [PubMed: 1373145]
29. Chen YP, et al. “Inside-out” signal transduction inhibited by isolated integrin cytoplasmic domains. J Biol Chem. 1994; 269:18307–10. [PubMed: 8034576]
30. Parsons M, Messent AJ, Humphries JD, Deakin NO, Humphries MJ. Quantification of integrin receptor agonism by fluorescence lifetime imaging. J Cell Sci. 2008; 121:265–271. [PubMed: 18216331]
31. Tadokoro S, et al. Talin binding to integrin beta tails: a final common step in integrin activation. Science. 2003; 302:103–6. [PubMed: 14526080]
32. Montanez E, et al. Kindlin-2 controls bidirectional signaling of integrins. Genes Dev. 2008; 22:1325–1330. [PubMed: 18483218]
33. Harburger DS, Bouaouina M, Calderwood DA. Kindlin-1 and -2 directly bind the C-terminal region of beta integrin cytoplasmic tails and exert integrin-specific activation effects. J Biol Chem. 2009; 284:11485–11497. [PubMed: 19240021]
34. Ma YQ, Qin J, Wu C, Plow EF. Kindlin-2 (Mig-2): a co-activator of beta3 integrins. J Cell Biol. 2008; 181:439–446. [PubMed: 18458155]
35. Gerlach B, et al. Linear ubiquitination prevents inflammation and regulates immune signalling. Nature. 2011; 471:591–596. [PubMed: 21455173]

36. Ikeda F, et al. SHARPIN forms a linear ubiquitin ligase complex regulating NF-kappaB activity and apoptosis. Nature. 2011; 471:637–641. [PubMed: 21455181]
37. Tokunaga F, et al. SHARPIN is a component of the NF-kappaB-activating linear ubiquitin chain assembly complex. Nature. 2011; 471:633–636. [PubMed: 21455180]
38. Soderberg O, et al. Direct observation of individual endogenous protein complexes in situ by proximity ligation. Nat Methods. 2006; 3:995–1000. [PubMed: 17072308]
39. Tuomi S, et al. PKCepsilon regulation of an alpha5 integrin-ZO-1 complex controls lamellae formation in migrating cancer cells. Sci Signal. 2009; 2:ra32. [PubMed: 19567915]
40. Askari JA, et al. Focal adhesions are sites of integrin extension. J Cell Biol. 2010; 188:891–903. [PubMed: 20231384]
41. Liang Y, Seymour RE, Sundberg JP. Inhibition of NF-kappaB signaling retards eosinophilic dermatitis in SHARPIN-deficient mice. J Invest Dermatol. 2011; 131:141–149. [PubMed: 20811394]
42. Seymour RE, et al. Spontaneous mutations in the mouse Sharpin gene result in multiorgan inflammation, immune system dysregulation and dermatitis. Genes Immun. 2007; 8:416–421. [PubMed: 17538631]
43. Tokunaga F, et al. Involvement of linear polyubiquitylation of NEMO in NF-kappaB activation. Nat Cell Biol. 2009; 11:123–132. [PubMed: 19136968]
44. Wegener KL, et al. Structural basis of integrin activation by talin. Cell. 2007; 128:171–182. [PubMed: 17218263]
45. Millon-Fremillon A, et al. Cell adaptive response to extracellular matrix density is controlled by ICAP-1-dependent beta1-integrin affinity. J Cell Biol. 2008; 180:427–441. [PubMed: 18227284]
46. Nevo J, et al. Mammary-derived growth inhibitor (MDGI) interacts with integrin alpha-subunits and suppresses integrin activity and invasion. Oncogene. 2010
47. Clark AJ, Neil C, Gusterson B, McWhir J, Binas B. Deletion of the gene encoding H-FABP/MDGI has no overt effects in the mammary gland. Transgenic Res. 2000; 9:439–44. [PubMed: 11206972]
48. Legate KR, Wickstrom SA, Fassler R. Genetic and cell biological analysis of integrin outside-in signaling. Genes Dev. 2009; 23:397–418. [PubMed: 19240129]
49. He L, Ingram A, Rybak AP, Tang D. Shank-interacting protein-like 1 promotes tumorigenesis via PTEN inhibition in human tumor cells. J Clin Invest. 2010; 120:2094–2108. [PubMed: 20458142]
50. Landgraf K, et al. Sipl1 and Rbck1 are novel Eya1-binding proteins with a role in craniofacial development. Mol Cell Biol. 2010; 30:5764–5775. [PubMed: 20956555]
51. Gustin JA, Maehama T, Dixon JE, Donner DB. The PTEN tumor suppressor protein inhibits tumor necrosis factor-induced nuclear factor kappa B activity. J Biol Chem. 2001; 276:27740–27744. [PubMed: 11356844]
52. Kilpinen S, et al. Systematic bioinformatic analysis of expression levels of 17,330 human genes across 9,783 samples from 175 types of healthy and pathological tissues. Genome Biol. 2008; 9:R139. [PubMed: 18803840]
53. O'Toole TE, et al. Modulation of the affinity of integrin alpha IIb beta 3 (GPIIb-IIIa) by the cytoplasmic domain of alpha IIb. Science. 1991; 254:845–7. [PubMed: 1948065]
54. Rantala JK, et al. A cell spot microarray method for production of high density siRNA transfection microarrays. BMC Genomics. 2011; 12:162. [PubMed: 21443765]
55. Kraemer A, et al. Dynamic interaction of cAMP with the Rap guanine-nucleotide exchange factor Epac1. J Mol Biol. 2001; 306:1167–1177. [PubMed: 11237625]
56. Clark K, et al. A specific alpha5beta1-integrin conformation promotes directional integrin translocation and fibronectin matrix formation. J Cell Sci. 2005; 118:291–300. [PubMed: 15615773]
57. Hogan, B. Manipulating the Mouse Embryo: A Laboratory Manual. Cold Spring Harbor Laboratory Press; Cold Spring Harbor, New York: 1986.
58. Laukaitis CM, Webb DJ, Donais K, Horwitz AF. Differential dynamics of alpha 5 integrin, paxillin, and alpha-actinin during formation and disassembly of adhesions in migrating cells. J Cell Biol. 2001; 153:1427–40. [PubMed: 11425873]

59. Caswell PT, et al. Rab25 associates with alpha5beta1 integrin to promote invasive migration in 3D microenvironments. Dev Cell. 2007; 13:496–510. [PubMed: 17925226]

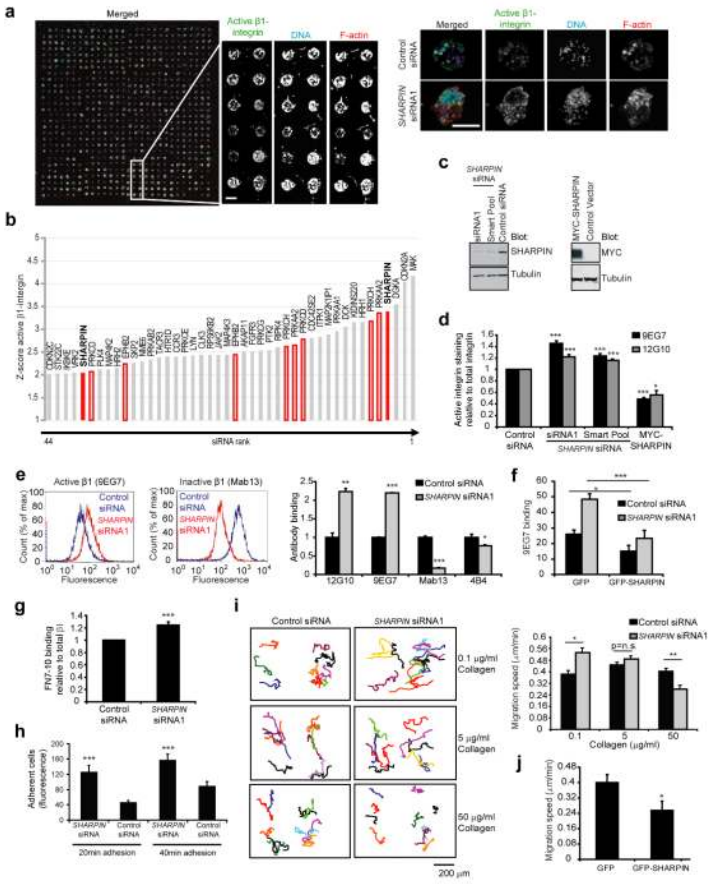

Fig. 1. SHARPIN is an inhibitor of β1-integrin activity

(**a**) siRNA screen for endogenous integrin inhibitors with prostate cancer cells (PC3) using a cell spot microarray (CSMA) technique. Shown are representative images of array spots stained as indicated (Scale bar 0.5 mm). On the right, control and *SHARPIN* siRNA positions are shown at higher magnification. (**b**) Z-score plot for active integrin labelling (mAb 12G10 normalized against DNA label DAPI) of the 44 highest scoring siRNAs. Red indicates siRNAs for those genes in which both individual siRNAs significantly increased integrin activity. (**c**) PC3 cells were transfected as indicated and analyzed with Western blotting (uncropped blots are shown in Supplementary Fig. S5). (**d**) ScanR microscopy analysis of PC3 cells transfected as in (c) and stained with two β1-integrin active epitope (9EG7 and 12G10) and one total β1-integrin antibodies (K20; shown in Supplementary Fig. S2a). Shown are mean fluorescence intensities (MFI) of 12G10 and 9EG7 relative to K20 (n=3). Value 1.0 is assigned to control siRNA treated cells. (**e**) FACS analysis of PC3 cells transfected as indicated and stained for surface levels of active (9EG7 and 12G10) or inactive (Mab13 and 4B4) β1-integrins. Shown are representative histograms and the MFI. The MFI in the control transfected cells is set to 1.0 for each antibody, n=4. (**f**) FACS analysis of 9EG7 labelling from PC3 cells double transfected with siRNAs and plasmids expressing siRNA-resistant GFP-SHARPIN or GFP alone. Shown are the MFI, n=3. (**g**) Binding of fibronectin (FN7-10 fragment) to control and *SHARPIN* silenced cells was analyzed using FACS. Staining intensities were normalized against total β1-integrin levels (n=3). (**h**) Adhesion of PC3 cells, transfected as indicated, to fibronectin for the indicated times was scored using PI stain (n=3). (**i**) Control and *SHARPIN* siRNA1 transfected PC3 cells adhering to the indicated concentrations of collagen I were scratch-wounded and analyzed using time-lapse microscopy for 15 hours. Shown are representative cell-tracks and

quantitation of the migration speed (n=100 cells). (**j**) Migration on plastic of PC3 cells transfected with GFP or GFP-SHARPIN, n=174 cells.
All numeric data are mean±SEM, * $p<0.05$, ** $p<0.01$, *** $p<0.001$, n.s.= not significant.

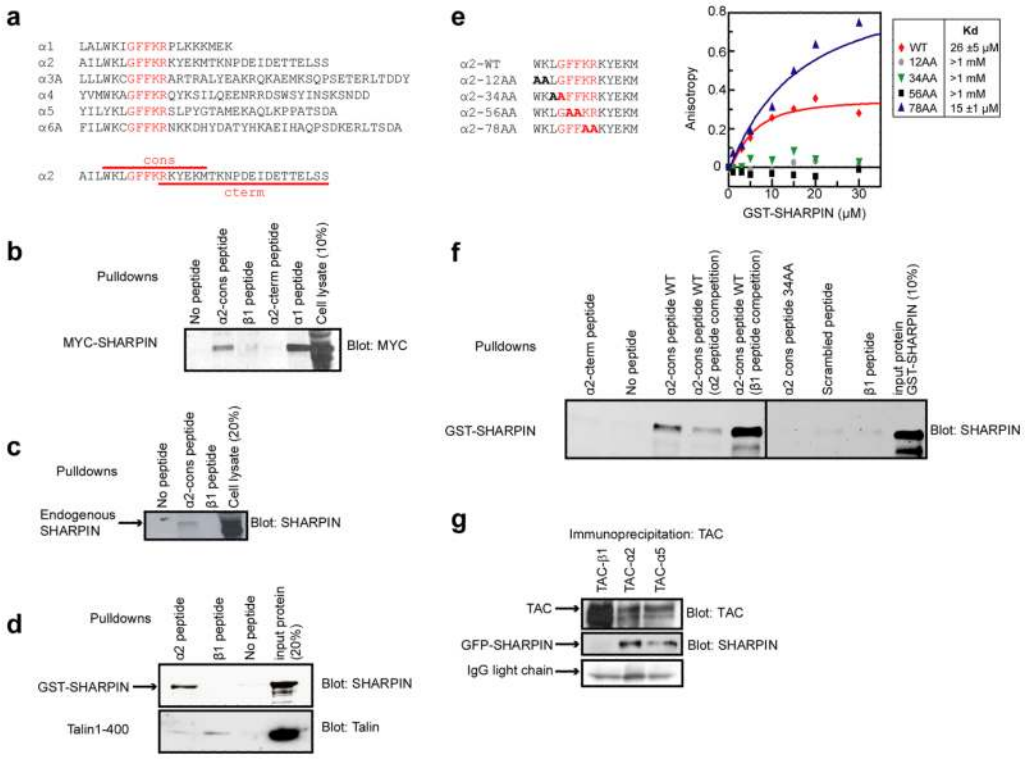

Fig. 2. SHARPIN interacts with the conserved membrane proximal segment of integrin α-tails

(**a**) Alignment of several C-terminal cytoplasmic domains of α-integrins. The conserved membrane-proximal (cons) and the c-terminal (cterm) peptides of α2-integrin used in this study are also indicated. (**b**–**d**) Streptavidin-bead pull-down assays with the indicated biotinylated integrin cytoplasmic-tail peptides or beads alone (no peptide) (b) from MYC-SHARPIN transfected (uncropped blot is shown in Supplementary Fig. S5) and (c) non-transfected PC3 cell extracts (uncropped blot is shown in Supplementary Fig. S5) or (d) with recombinant GST-SHARPIN and recombinant Talin1–400 fragment. (**e**) Fluorescence polarization based titration of GST-SHARPIN binding to the integrin peptides. Representative binding curves to wild-type (WT) and alanine mutated α2-tails and the Kd-values (mean±SEM, n=4) are shown. (**f**) Streptavidin-bead pull-down assay with recombinant GST-SHARPIN and the indicated biotinylated peptides in the presence or absence of competing peptides (10-fold excess soluble, unlabelled peptides). Uncropped blot is shown in Supplementary Fig. S5. (**g**) Lysates from GD25 cells (β1-integrin null), co-transfected with GFP-SHARPIN and interleukin receptor TAC-subunit fused to the indicated integrin cytoplasmic tails were immunoprecipitated with anti-TAC antibody and blotted as indicated (uncropped blots are shown in Supplementary Fig. S5).

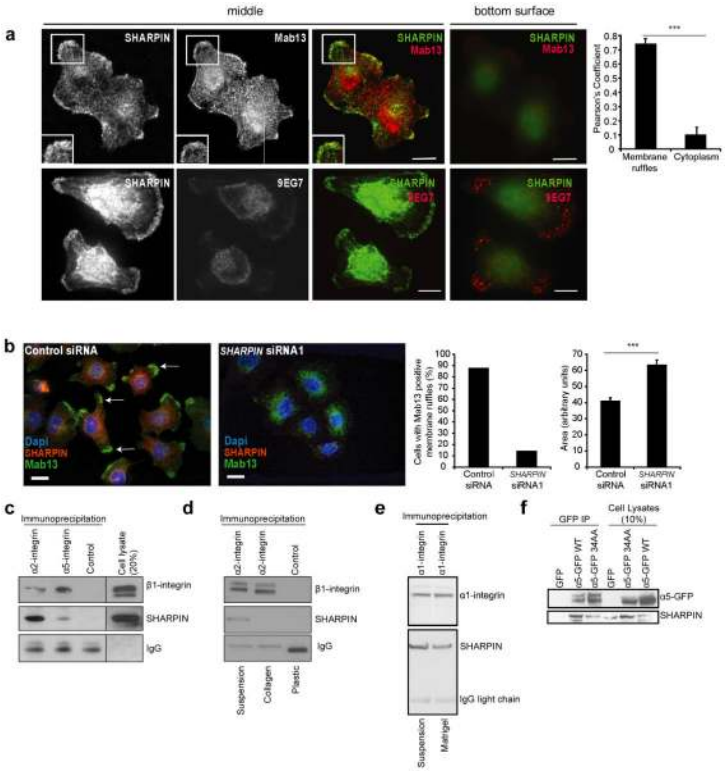

Fig. 3. SHARPIN colocalizes with inactive β1-integrins in membrane ruffles and associates with them in cells

(**a**) Non-transfected NCI-H460 cells stained as indicated. Shown are confocal slices from the middle of the cell and from the bottom surface. Scale bar 10 μm. The insets show higher magnifications. The graph shows analysis of SHARPIN and Mab13 co-localization (Pearson's correlation coefficient, n=12). (**b**) Control and *SHARPIN* siRNA transfected NCI-H460 cells stained as indicated. The arrows indicate Mab13-positive membrane ruffles. Scale bar 10 μm. The graphs show quantitation of the percentage of cells with Mab13 positive membrane ruffles (n= 43 cells) and the cell area (n=48 cells) for control and *SHARPIN* siRNA transfected cells. (**c**) Co-immunoprecipitations of α-integrins and SHARPIN in non-transfected PC3 cells grown on plastic (uncropped blots are shown in Supplementary Fig. S5). (**d**–**e**) Co-immunoprecipitations of α2- (**d**) or α1-integrin (**e**) and SHARPIN in non-transfected PC3 cells kept in suspension or plated on the indicated substrates (collagen type I for α2-integrin and collagen type IV containing Matrigel for α1-integrin). Uncropped blots are shown in Supplementary Fig. S5. (**f**) Co-immunoprecipitations of α5-integrin (WT or 34AA mutant) and SHARPIN in PC3 cells transfected with the indicated plasmids (note the higher amount of SHARPIN in the α5-GFP34AA lysates). Uncropped blots are shown in Supplementary Fig. S5.
All numeric data are mean±SEM, *** $p<0.001$.

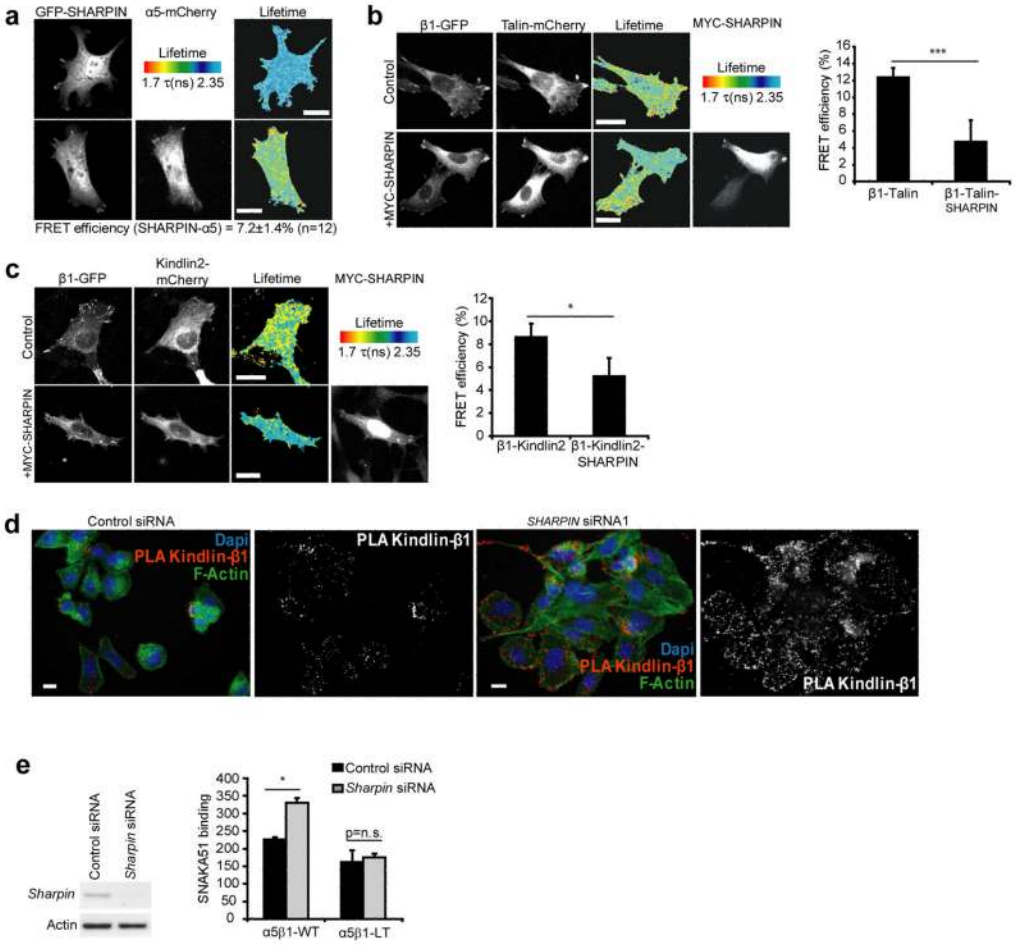

Fig. 4. SHARPIN directly interacts with β1-integrins in cells and inhibits recruitment of Talin and Kindlin to β1-integrins

(**a**) PC3 cells transfected with GFP-SHARPIN with (lower row) or without (upper row) α5-integrin-mcherry subjected to FRET analysis by FLIM. Lifetime images mapping spatial FRET in cells are depicted using a pseudo-colour scale (blue, normal lifetime; red, FRET (reduced lifetime)). Scale bars 10 μm. (**b**–**c**) β1−/− MEF cells transfected with (b) β1-GFP and mcherry-Talin or (c) β1-GFP and mcherry-Kindlin2 (the predominant Kindlin isoform expressed in fibroblasts) in combination with an empty control plasmid or MYC-SHARPIN and subjected to FRET analysis by FLIM (as in a), n=12–19 cells. Note the dose-dependent effect of MYC-SHARPIN in the two cells shown in (b). Scale bars 10 μm. (**d**) PLA between β1-integrin and Kindlin in SHARPIN or control silenced PC3 cells. Scale bar 10 μm. (**e**) RT-PCR analysis of *Sharpin* and actin mRNA levels in β1-null GD25 mouse cells transfected with *Sharpin* siRNA or control siRNA. Cells double-transfected with the indicated siRNAs and plasmids expressing either β1-CFP-WT and α5-YFP-WT or legs together (LT) restrained mutants β1-CFP-LT and α5-YFP-LT were stained with an antibody recognizing active human α5β1 integrin (SNAKA51) and analyzed with FACS. Shown are mean fluorescence intensities of SNAKA51 staining of CFP/YFP double-positive cells (n=3).

All numeric data are mean±SEM, * $p<0.05$, *** $p<0.001$, n.s.=not significant.

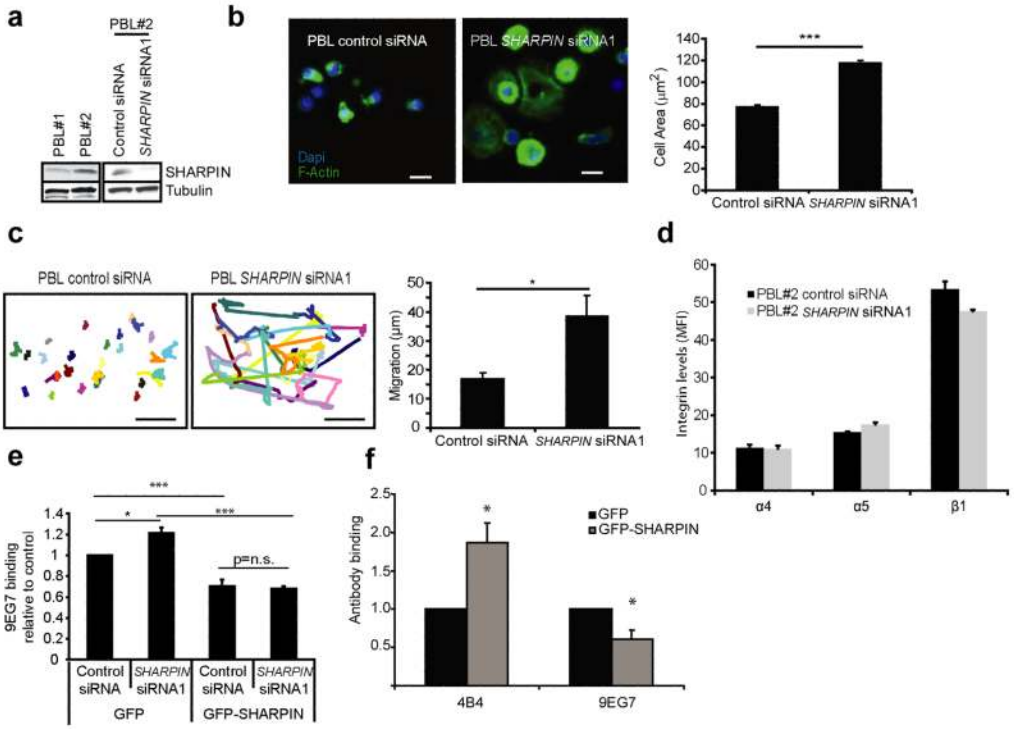

Fig. 5. SHARPIN inhibits β1-integrin activity in primary human leukocytes

(**a**) SHARPIN and tubulin levels in freshly isolated PBL from two individuals and in PBL (#2) silenced with control or *SHARPIN* siRNA1 for 48 h. (**b**) Spreading of *SHARPIN* siRNA1 or control siRNA transfected human PBL on 1 μg/ml fibronectin after 1 h. The cells were stained with DAPI (blue, nuclei) and phalloidin (green), and the cell areas (green) quantitated by microscopy (mean±SEM, n=1671–3681 cells). Scale bar 10 μm. (**c**) Migration of *SHARPIN* siRNA1 or control siRNA transfected human PBL on fibronectin (n=49 cells). Representative migration tracks and quantitation of the migration distance are shown. Scale bar 10 μm. (**d**) SHARPIN and control silenced human PBLs were stained for α4- and α5-integrin and total β1-integrin (K20) (n=3). (**e**) FACS staining of cell surface 9EG7 levels in PBL (#2) transfected with control or *SHARPIN* siRNA1 together with GFP or siRNA-resistant GFP-SHARPIN. Value 1.0 was assigned to control siRNA and GFP transfected cells) (n=3). (**f**) FACS analysis of cell surface levels of active (9EG7) and inactive (4B4) β1-integrin in human PBL transfected with GFP or GFP-SHARPIN from 3 independent transfections. Binding in GFP transfected cells is assigned value 1.0.
All numeric data are mean±SEM, * $p<0.05$, *** $p<0.001$, n.s.=not significant.

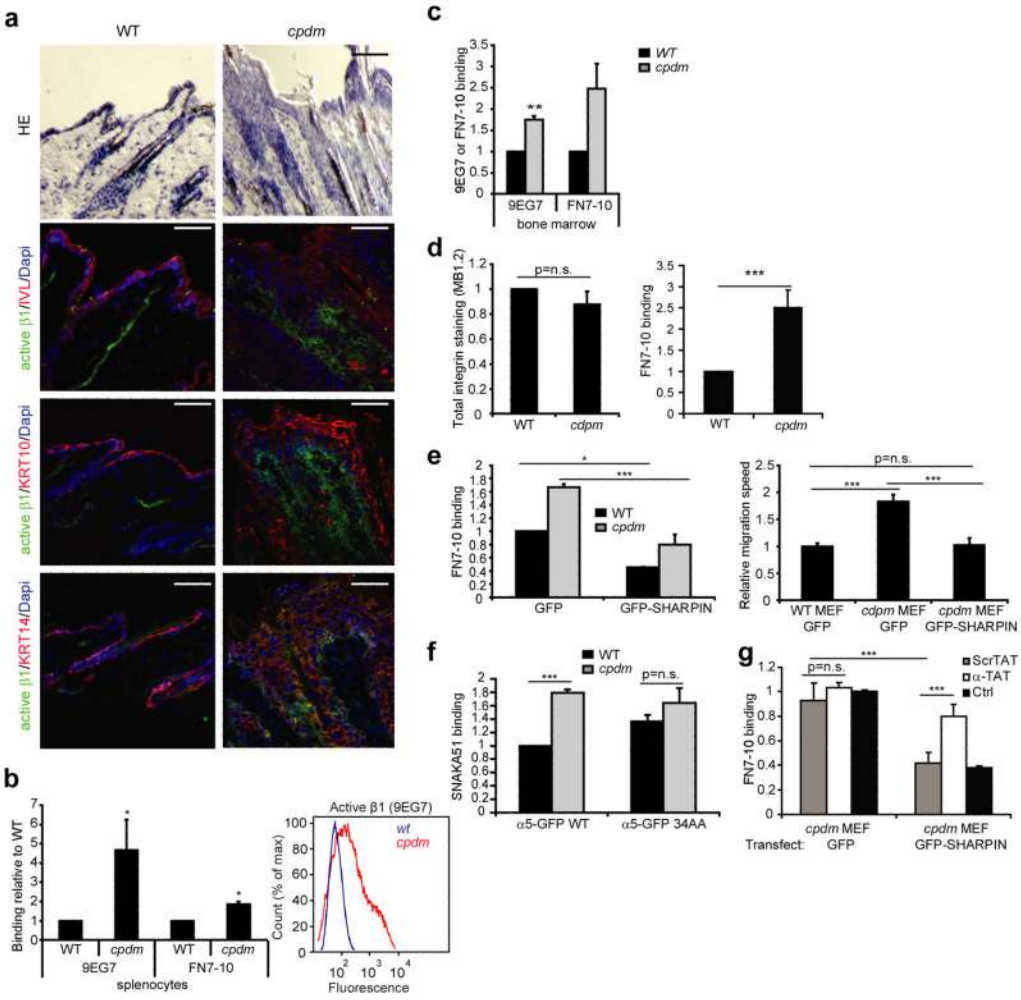

Fig. 6. Loss of SHARPIN correlates with increased β1-integrin activity *in vivo*

(**a**) HE-stainings and immunofluorescence co-stainings of active β1-integrin and involucrin (IVL), keratin 10 (KRT10) and keratin 14 (KRT14) of skin samples from wild-type (WT) and SHARPIN null (*cpdm*) mice. DAPI was used to stain nuclei. Scale bars 50 μm. (**b**) Primary splenocytes isolated from WT and *cpdm* mice were analyzed using FACS for binding to fibronectin (FN7-10 fragment) or 9EG7 antibody (n=6 mice/genotype). Shown are the mean fluorescence intensities relative to WT splenocytes, and representative histograms. (**c**) Binding of fibronectin (FN7-10 fragment) and 9EG7 to WT and *cpdm* primary leucocytes (bone marrow cells) was analyzed using FACS (n=3 mice/genotype). Binding to WT cells is assigned value 1.0. (**d**) FACS analysis of total β1-integrin levels on the surface of WT and *cpdm* MEFs (left). Binding of fibronectin (FN7-10 fragment) to WT and *cpdm* MEFs (right) was analyzed using FACS (n=4). Binding to WT cells is assigned value 1.0. (**e**) Binding of fibronectin (FN7-10 fragment) to MEFs from WT and *cpdm* mice transfected with GFP or GFP-SHARPIN was analyzed using FACS. The staining intensities are shown relative to WT MEFs transfected with GFP (n=3). Analysis of migration speed of WT and *cpdm* MEFs transfected with GFP or GFP-SHARPIN (n>25 cells). (**f**) MEFs from WT and *cpdm* mice were transfected with full-length α5-GFP WT or α5-GFP 34AA mutant and the α5β1-integrin activity was analysed with SNAKA51 antibody using FACS. Shown are mean fluorescence intensities of SNAKA51 stainings relative to GFP intensity (the intensity of WT MEFs expressing WTα5 is defined as 1.0) (n=3). (**g**) Binding of fibronectin

(FN7-10 fragment) to *cpdm* MEFs transfected with GFP or GFP-SHARPIN in the presence or absence of membrane-permeable SHARPIN binding α-tail peptide (α1-TAT) or scramble peptide (ScrTAT) was analyzed using FACS (n=3). Ctrl, control without peptides.
All numeric data are mean±SEM, * $p<0.05$, ** $p<0.01$, *** $p<0.001$, n.s.=not significant.